Published in final edited form as:
Thromb Haemost. 2011 June ; 105(6): 1032–1045. doi:10.1160/TH11-01-0029.

A novel family of RGD-containing disintegrin (Tablysin-15) from the salivary gland of the horsefly *Tabanus yao* targets integrins $\alpha_{IIb}\beta_3$ and $\alpha_V\beta_3$ and inhibits platelet aggregation and angiogenesis

Dongying Ma[1,*], **Xueqing Xu**[2,*], **Su An**[1,4,*], **Huan Liu**[1], **Xuening Yang**[1], **John F. Andersen**[2], **Yipeng Wang**[1], **Fuyuki Tokumasu**[3], **José M. C. Ribeiro**[2], **Ivo M. B. Francischetti**[2,¶], and **Ren Lai**[1,¶]

[1]Key Laboratory of Animal Models and Human Disease Mechanisms, Kunming Institute of Zoology, Chinese Academy of Sciences, Kunming, Yunnan, China

[2]Vector Biology Section, Laboratory of Malaria and Vector Research, National Institute of Allergy and Infectious Diseases, National Institutes of Health, Bethesda, Maryland, USA

[3]Biochemical and Biophysical Parasitology Section, Laboratory of Malaria and Vector Research, National Institute of Allergy and Infectious Diseases, National Institutes of Health, Bethesda, Maryland, USA

[4]School of Life Sciences, University of Science and Technology of China, Hefei, Anhui, China

Abstract

A novel family of RGD-containing molecule (Tablysin-15) has been molecularly characterized from the salivary gland of the hematophagous horsefly *Tabanus yao*. Tablysin-15 does not share primary sequence homology to any disintegrin discovered so far, and displays an RGD motif in the N-terminus of the molecule. It is also distinct from disintegrins from Viperidae since its mature form is not released from a metalloproteinase precursor. Tablysin-15 exhibits high affinity for platelet $\alpha_{IIb}\beta_3$ and endothelial cell $\alpha_v\beta_3$ integrins, but not for $\alpha_5\beta_1$ or $\alpha_2\beta_1$. Accordingly, it blocks endothelial cell adhesion to vitronectin (IC_{50} ~ 1 nM) and marginally to fibronectin (IC_{50} ~ 1 μM), but not to collagen. It also inhibits FGF-induced endothelial cell proliferation, and attenuates tube formation *in vitro*. In platelets, Tablysin-15 inhibits aggregation induced by collagen, ADP and convulxin, and prevents static platelet adhesion to immobilized fibrinogen. In addition, solid-phase assays and flow cytometry demonstrates that $\alpha_{IIb}\beta_3$ binds to Tablysin-15. Moreover, immobilized Tablysin-15 supports platelet adhesion by a mechanism which was blocked by anti-integrin $\alpha_{IIb}\beta_3$ monoclonal antibody (*e.g.* abciximab) or by EDTA. Furthermore, Tablysin-15 dose-dependently attenuates thrombus formation to collagen under flow, without affecting platelet adhesion to collagen fibrils. Consistent with these findings, Tablysin-15 displays antithrombotic properties *in vivo* suggesting that it is a useful tool to block $\alpha_{IIb}\beta_3$, or as a prototype to develop antithrombotics. The RGD motif in the unique sequence of Tablysin-15

[¶]Correspondence: Ren Lai, Key Laboratory of Animal Models and Human Disease Mechanisms, Kunming Institute of Zoology, Chinese Academy of Sciences, Kunming 650223, Yunnan, China; rlai@mail.kiz.ac.cn; or Ivo M.B. Francischetti, Vector Biology Section Laboratory of Malaria and Vector Research, NIAID, National Institutes of Health, Bethesda, Maryland, USA. ifrancischetti@niaid.nih.gov.
[*]These authors contributed equally to this paper.

Contribution: R.L. and I.M.B.F. provided experimental design and reagents, analyzed the data, and wrote the paper; D.M., X.X., S.A, H.L., X.Y., J.F.A., Y.W., and F.T. performed the experiments; J.M.C.R. provided reagents and analyzed the data. X.X. wrote the paper.

Conflict-of-interest disclosure: The authors have no conflicting financial interests.

represents a novel template for studying the structure-function relationship of the disintegrin family of inhibitors.

Keywords

hematophagy; blood-sucking; disintegrin; thrombosis; sialogenins

Introduction

Integrins are heterodymeric membrane glycoproteins composed of noncovalently associated α and β subunits that promote cell attachment and migration on the surrounding extracellular matrix. Many integrins bind to their extracellular ligands through the recognition of the tripeptide Arg-Gly-Asp (RGD). This motif is present in several protein components of extracellular matrix, including vitronectin, fibronectin, osteopontin, and fibrinogen. Although different ligands can bind to the same integrin, sequences flanking the RGD peptide are reported to be important for integrin selectivity. Integrin ligation by its own natural ligands promotes intracellular signaling by kinases and adaptor proteins and by activating a number of intracellular mediators that ultimately lead to cell migration, survival, and invasion (1–3). Of note, much of the mechanism of action of integrins has been revealed by peptides from viper venoms – the disintegrins – which reportedly blocks integrin interaction (*e.g.* αIIbβ3) with its physiological ligand (e.g. fibrinogen) (4).

Disintegrins are a family of small cysteine-rich polypeptides which display series of biological functions associated with cell-cell interaction, cell adhesion and migration and angiogenesis (5–6). Disintegrins are commonly processed from PII or PIII metalloproteinase precursors through proteolytic processing and have tripeptide motifs RGD, KGD, WGD, VGD, MGD, RTS, KTS, ECD, among others, which confers binding specificity. Currently, disintegrins can be classified in four groups. The first group of short disintegrins displays 41–51 residues and four disulphide bonds, the second group contain approximately 70 amino acids and six cystine bonds while the third group includes disintegrins with approximately 84-residue polypeptide cross-linked by seven disulphide bridges. The fourth group is composed of homodimers or heterodimers with subunits of approximately 67 residues with ten cysteines involved in the formation of four intrachain disulphides and two interchain cystine linkages (7–11). Of note, disintegrins function and specificity depends on the appropriate pairing of cysteine residues which exposes the tripeptide inhibitory binding motif. This specificity is particularly relevant because integrins play a pivotal role in several physiological events such as platelet aggregation (12), neutrophil function (13) and endothelial cell adhesion and angiogenesis (14). Accordingly, disintegrins have been instrumental in the development of anti-platelets molecules and inhibitors of angiogenesis with potential therapeutic applications (15–17).

While snake venoms express toxins, saliva from blood-sucking arthropods express sialogenins (from the Greek *sialo*, saliva; *gen*, origin, source; and *ins* for proteins) (18). Sialogenins interfere with diverse functions of vertebrate biology, including immune system, vasodilation, blood coagulation and platelet aggregation (19). Among anti-platelet sialogenins, disintegrins have been molecularly and functionally characterized in ticks and leeches (20), but have not been discovered in mosquitoes, bugs, or flies (18–24). While investigating the diversity of antihemostatic molecules of the horsefly, we identified a novel platelet inhibitor from the salivary glands of *T. yao*. Tablysin-15 contains a unique sequence that displays an RGD domain in the N-terminus and effectively prevents platelet or endothelial function associated with integrin αIIbβ3 or αvβ3, respectively.

Methods

Horsefly collection

T. yao Macquart horseflies (about 60,000; average weight 0.17 g) were collected in Shanxi Province, China, from July 2004 to July 2008. Collections were performed between 17:00 and 20:00 during optimal weather (sunny, 30–35°C, no wind). All the flies were transported to the laboratory alive and then frozen and stored at −80°C.

Salivary gland dissection and salivary gland extract (SGE) preparation

As described in our previous work (25–26), horseflies were glued to the bottom of a Petri dish and placed on ice. They were then dissected under a microscope. The salivary gland was excised and transferred into 0.1 M phosphate buffered saline (PBS), pH 6.0, and kept in the same solution at −80°C. Horsefly salivary glands (60,000 pairs) were homogenized in 0.1 M PBS and centrifuged at 5000 *g* for 10 min. The supernatant was termed SGE and lyophilized.

Fractionation of SGE

As described in our previous work (25–26), the total lyophilized SGE sample was 4.1 g. The sample was divided into ten aliquots (aliquot of 0.41 g). The purification procedure of the target protein is illustrated in Figure 1. All purified interesting proteins from ten aliquots of SGE were pooled and subjected to further study.

SDS-PAGE analysis and protein concentration determinations

SDS-PAGE was performed under reduced and non-reduced conditions. Protein samples were loaded onto a 15% polyacrylamide gel. Protein bands were observed after using Coomassie blue staining. Protein concentration was determined by a protein assay kit (Bio-Rad, Hercules, CA) in which bovine serum albumin (BSA) was employed as a standard.

Structural analysis

Aa sequences of the N-terminus and partial interior peptide fragments recovered from trypsin hydrolysis were determined by automated Edman degradation on a pulsed liquid-phase sequencer (model 491; Applied Biosystems, Fullerton, CA).

cDNA cloning

cDNA synthesis and cDNA library construction were conducted according to our previous methods (25–26). The specific primer (5′-(C/G)GG (T/C)AG (C/T)TT GTC (G/C)CC GGA GTA-3) in the sense direction, designed according to the peptide sequences determined by Edman degradation, and primer II A (5′-AAGCAGTGGTATCAACGCAGAGT-3′) in the antisense direction were used in PCR reactions. The DNA polymerase was Advantage polymerase from Clontech (Palo Alto, CA). The PCR conditions were as follows: 2 min at 94°C, followed by 30 cycles of 10 sec at 92°C, 30 sec at 50°C, and 40 sec at 72°C. DNA sequencing was performed on an Applied Biosystems DNA sequencer, model ABI PRISM 377.

Expression of Tablysin-15

The coding region, including restriction enzyme sites for Tablysin-15, was isolated from a salivary gland cDNA library of *T. yao*. The forward primer was 5′-TA***GGATCC***GTTAACT ACTGTAGATTACCCTGCCG-3′ and the reverse primer was 5′-GG***AAGCTT***AGTTAGA TTTATTAGGGTCGATAGG-3′. PCR was performed by running 30 cycles with a temperature profile of 30 s at 95°C, 30 s at 57°C, and 60 s at 72°C. The purified PCR

product was digested with *BamH*I and *Hin*dIII and ligated into the pET-32a(+) plasmid at the corresponding restriction sites. Expression, purification, and refolding of the recombinant His-tagged protein were performed according to the manufacturer's instruction (Novagen, Madison, WI). Briefly, transformed cells of *Escherichia coli* strain BL21 (DE3) were grown at 37°C in Luria–Bertani medium supplemented with ampicillin (100 μg/mL) to a cell density of A_{660nm} = 0.6. After induction of protein expression with 0.4 mM IPTG, cells were disrupted by sonication and inclusion bodies were solubilized in 20 mM Tris–HCl, pH 7.9, with 6 M urea. The lysate was centrifuged and the supernatant applied to a Ni-NTA resin (Invitrogen, San Diego, CA) equilibrated with the same buffer. Recombinant proteins were released by enterokinase from the fusion protein. They were purified from the digestive mixture by AKTA Mono S cationic exchange column.

Platelet preparation and labeling with calcein-AM

Human platelet-rich plasma (PRP) was obtained by plateletpheresis and diluted to 2×10^5 platelets/μL in Tyrode's buffer (137 mM NaCl, 2 mM KCl, 0.3 mM NaH_2PO_4, 12 mM $NaHCO_3$, 5.5 mM glucose, 0.35% BSA, 1 mM $MgCl_2$, and pH 7.4). To prepare washed platelets, PRP was centrifuged at 500 *g* for 10 min at room temperature in the presence of apyrase (0.2 U/ml) and EDTA (5 mM) (27). The pellets were suspended in Tyrode's buffer supplemented with apyrase and EDTA, and after washing and centrifugation, platelets were resuspended in Tyrode's buffer. Platelet aggregation was monitored by light transmission in an Chrono-Lumi platelet aggregometer (Chronol-Log, Havertown, PA) with continuous stirring at 37°C. In some experiments, washed platelets were incubated with 2 μM of calcein-AM for 30 min (in the presence of apyrase and EDTA) followed by centrifugation as above. Convulxin was purified as reported (27).

Thrombus formation under flow conditions

Glass slides were coated with fibrillar collagen (500 μL, 100 μg/mL in PBS; Chrono-Log Corp., Haverton, PA) for 15 min, washed in PBS, pH 7.4, and incubated overnight with denatured (65°C, 1 hr) BSA (7 mg/mL). Coated slides were placed in the bottom of the parallel plate flow chamber (Glycotech, Rockville, MD), and a silicone rubber gasket determined the flow path height of 254 μm, as described (28). Anticoagulated blood (50 μM d-phenylalanyl-l-prolyl-l-arginine chloromethyl ketone dihydrochloride) was mixed with Tablysin-15 and aspirated using a 10 ml syringe (slit tip, BD biosciences 301604). Then, Tablysin-15 mixed blood was perfused using an infusion/withdrawal pump with multispeed transmission (model 940; Harvard Apparatus, Dover, MA) through the flow chamber at a flow rate of 0.65 mL/min (position 5), producing a shear rate of 1,500 s^{-1}. Blood was perfused for 240 s followed by immediate perfusion with Tyrode/BSA (0.65 mL/min) for 120 s, and slides were subsequently washed by immersion in Tyrode/BSA (3 × 50 ml in Falcon tubes in tandem). Slide borders were touched using Precision Wipes to remove extract liquids, and mounted. Differential interference contrast images were obtained with a Leica DMI 6000 microscope (Leica Microsystems, Inc., Bannockburn, IL) using 100× objective with NA = 1.30, and an ORCA ER digital camera (Hamamatsu Photonic Systems, Bridgewater, NJ). Image acquisition and the digital camera were controlled by ImagePro 5.1 software (Media Cybernetics, Silver Spring, MD). Extent of thrombus formation was expressed as percent area covered by thrombus. Platelet adhesion to collagen, which was characterized by single platelets which adhered to fibrillar collagen at 3 μM of Tablysin-15, was not considered thrombus formation despite evident area coverage.

Inhibition of platelet adhesion by Tablysin-15

Platelet adhesion was measured using a modified method originally described by McLane, et al (24). Briefly, U-shapped Microfluor 2 black high-affinity 96-well plates form fluorescence applications (Thermo Electron Co., Milford, MA, USA) were coated overnight

at 4°C with 1 μg/well of bovine fibronectin (F1141; Sigma), 100 μg/well of human fibrinogen (F3879; Sigma), 2 μg/well of soluble nonfibrillar collagen type I (BD Bioscience, San José, CA), 2 μg/well of insoluble fibrillar Horm collagen composed of type I and III (Chrono-Log Corp.), or Tablysin-15 (at indicated amounts). Unbound proteins were subsequently removed by plate inversion and washed three times with 200 μL of PBS. The wells were blocked with 200 μL of PBS containing 2% BSA for 1 h and washed three times with 200 μL of PBS. Fifty μL of calcein-labeled platelets (2×10^5/μl) were incubated for 30 min at 37°C with Tablysin-15, 20 mM EDTA, or 0–20 μg/mL of anti-integrin αIIbβ3 (Abciximab, ReoPro, Centocor BV, Leiden, The Netherlands). Then, the mixture was added to each well, and the plate was incubated under static conditions for 2 hours at 37°C. Nonadherent platelets were removed by plate inversion, and the wells were washed three or four times with 200 μL of Tyrode/BSA. Adherent plates were detected using a dual-scanning microplate spectrofluorometer (Germini XPS; Molecular Devices, Sunnyvale, CA) at 490 nm of excitation wavelength and 520 nm emission wavelength. Results were estimated as percent inhibition, considering 100% platelet adhesion in the presence of PBS, and 0% adhesion in the presence of EDTA (20 mM). All experiments were performed in quintuplicates.

αIIbβ3 binding to Tablysin-15

Tissue culture-treated flat-bottom polystyrene plates (3596, Corning Incorporated, NY) were coated with increasing concentrations of purified Tablysin-15, fibrinogen, SVEP-E2 protein (unrelated salivary protein expressed in *E.coli*, negative control), or a 1% BSA (v/v) diluted in 0.1 M sodium carbonate, pH 9.5 at 4°C overnight. After unbound proteins were removed by washing three times with TACTS (20 mM Tris, 0.15 M NaCl, pH 7.5, 2 mM $CaCl_2$, 0.05% Tween 20) wells were blocked with 1% BSA in TACTS for 1 h. Purified human platelet αIIbβ3 (50 μl, 20 μg/ml in TACTS) (Enzyme Research Laboratories, Southbend, IN) diluted in TACTS containing 0.5% BSA was added to each well. After 2-h incubation, the wells were washed in TACTS followed by addition of mouse anti-human integrin β3 antibody (1:2000, CBL479; Millipore, Bedford, MA) in 1:2000 in TACTS containing 0.5% BSA. Following 1-h incubation at 37°C, wells were washed (TACTS) and anti-mouse IgG conjugated to alkaline phosphatase (1:2000, A3562; Sigma) in TACTS containing 0.5% BSA was added to the wells. Before adding the stabilized *p*-nitrophenyl phosphate liquid substrate (N7653; Sigma), wells were washed three times with TACTS. After 30 min of substrate conversion, the reaction was stopped with 3 M NaOH, and absorbance was read at 405 nm using a Thermomax microplate reader (Molecular Devices). Net specific binding was obtained by subtracting optical density values from wells coated only with BSA from the total binding measured as described above. Binding was not detected in the absence of αIIbβ3. All experiments were performed in triplicate.

Tablysin-15 binding to platelet $\alpha_{IIb}\beta_3$ by flow cytometry

Platelet $\alpha_{IIb}\beta_3$ occupancy kits (Biocytex, Marseille, France) were used to quantify the total number of platelet $\alpha_{IIb}\beta_3$ receptors and the number of free $\alpha_{IIb}\beta_3$ receptors (free of aggregation-inhibitory molecules) by flow cytometry (29–30). Briefly, whole blood was collected from healthy volunteers who had not taken any antiplatelet agent in the previous 7 days. The platelet-rich plasma (PRP) was diluted to 2×10^5 platelets/μl with the platelet poor plasma (PPP). Aliquots of 50 μl PRP were treated with 20 μl recombinant Tablysin-15 (0–22.5 μg /ml) for 60 min. Aliquots of each dilution were incubated with monoclonal antibody 1 (mAb) and mAb2 (10 μg/ml) at 37°C for 30 min. The samples were then immuno-labeled, fluorescent stained and finally analyzed by flow cytometry (FACSvantage; Becton Dickinson, Oxford, UK) at 488 nm excitation. Platelet populations were gated according to their forward and side light scatter. Histograms were generated using 10,000 counts and geometric mean fluorescence was calculated using the CELLQUEST software of

the FACScan system (Becton Dickinson). The binding of an isotypic control antibody was taken as nonspecific binding and was subtracted from the observed geometric mean fluorescence. The selected Mean Fluorescence Intensity (MFI) indicated the number of platelet $\alpha_{IIb}\beta_3$ receptor.

Human dermal microvascular MVEC culture

Adult MVEC were purchased from Clonetics (San Diego, CA) and grown at 37°C, 5% CO2 in T-25 flasks in the presence of EBM-2 Plus: EBM-2 containing 2% fetal bovine serum, and Single Quotes (h-fibroblast growth factor-B, vascular endothelial growth factor, R^3-insulin growth factor, ascorbic acid, h-epidermal growth factor, hydrocortisone plus gentamycin and amphotericin B). Trypsinization was performed using Reagent Pack (trypsin-EDTA, trypsin neutralization solution, and HBSS) according to the manufacturer instructions (Cambrex, MD).

MVEC adhesion to matrix proteins

Multimeric VTNC (Molecular Innovations, Southfield, MI), fibronectin (Sigma Co, Saint Louis), or soluble collagen III (BD Biosciences, Bedford, MA) were diluted to 20 μg/ml PBS (50 μl/well, 1 μg/well, in quintuplicate) were immobilized overnight at 4°C in Microfluor 2 black U-bottom high-binding 96-well plates for fluorescence applications (Thermo Electron Co., Milford, MA, USA). Wells were washed three times with PBS, blocked with BSA 2% (w/v) for two hours, and washed with PBS-BSA 0.3% (no additions). MVEC were trypsinized, and resuspended in EBM-2, 0.3% BSA (500,000/ml), without FBS or single quotes. Cells were loaded with calcein-AM (2 μM), for 45 minutes under rotation (at RT) and washed once. Cells were re-suspended in EBM-2, BSA 0.3% (no FBS or single quotes additions) to a concentration of 500,000/ml. Then, 50 μl of MVEC previously incubated with Tablysin-15 (0–3 μM) for 20 min at 37°C, 5% CO_2, were added to the matrix protein-coated plates (25,000 cells/well) and incubated for 90 minutes. Plates were then inverted and washed with EBM-2, BSA 0.3% (no FBS or single quotes) three or four times, and fluorescence was measured with excitation wavelength at 490 nm and emission wavelength at 520 nm using a Spectramax Gemini XPS Microfluor plate reader (Molecular Devices, Sunnyvale, CA, USA). Fluorescence produced by cells attached to each immobilized matrix protein in the absence of Tablysin-15 was set as 100% adhesion; adhesion to wells in the presence of EDTA (20 mM) was set as 0% adhesion. All experiments were performed in quintuplicates.

Proliferation assay kit

Cell proliferation assays were performed using the CellTiter 96 aqueous non-radioactive cell proliferation assay kit (Promega, Madison, WI). This assay uses MTS solution containing 3-(4,5-dimethylthiazol-2-yl)5-(3-carboxymethoxyphenyl)-2-(4-sulfophenyl)- 2H-tetrazolium) and phenazine methosulphate. MTS is bioreduced by cells into a formazan product soluble in tissue culture medium.

Cell proliferation assays

This was performed as described (31). In brief, after trypsinization, MVEC were seeded at 3.2×10^3/well in 96-well polystyrene tissue culture-treated plates (Corning Inc., Corning, NY) and grown for 1 day in the presence of EBM-2-Plus (EBM-2 containing FBS plus single quotes). In the next day, EBM-2 with additions was replaced by 200 μL of fresh EBM-2 supplemented with FBS (2%, v/v) and FGF (no other single quotes added) followed by addition of Tablysin-15 (0–3 μM). Three days latter, 40 μl of MTS solution was added to the wells and after 4 h at 37°C, absorbance at 490 nm was measured spectrophotometrically using a Versamax microplate reader equipped with the appropriate software (Molecular

Devices, San Diego, CA). Results were estimated as percent inhibition, considering 100% the MVEC growth in the presence of EBM-2 (FBS and FGF) and 0% growth in the presence of EBM-2 (no FBS, no single quotes). All experiments were performed in quintuplicates.

Tube Formation Assay

Tube formation assay was done as described with modifications (32). Ninety six wells flat bottom tissue culture plates (96-well; Corning, NY) were coated with 50 μl of growth factor-reduced Matrigel (BD Biosciences) and allowed to solidify at room temperature. One hundred μl of MVEC suspended in EBM-2 (no FBS or single quotes, supplemented with antibiotics and 0.3% BSA; at 5×10^5/ml) were incubated with Tablysin-15 at the concentrations indicated in the figure legends and added to each well. Plates were incubated at 37 °C, 5% CO_2 for 5–6 h, and formation was observed under an inverted microscope coupled to a digital camera (Axiovert 200; Carl Zeiss, Inc., Thornwood, NJ). Images were captured with AxioCamHR color camera (model 412–312) attached to the microscope.

Antithrombotic study by rat arteriovenous shunt thrombosis model

Male Wistar rats (180–220 g) were used for as rat arteriovenous shunt thrombosis model according to the method described by Sperzel and Huetter (33). Rats were anesthetized by intraperitoneal (*i.p.*) administration of ketamine (50 mg/kg) and xylazine (15 mg/kg). The left jugular vein and right common carotid artery were isolated and catheterized by a shunt catheter (American Health & Medical Supply International Corp., Scarsdale, NY). This catheter is composed of three parts including two 100-mm-long polyethylene (PE)-60 catheters, which were introduced into the blood vessels, and a 30-mm-long PE-160 catheter that is in the middle of the two PE-60 catheters. A rough nylon thread (60 mm in length and 0.26 mm in diameter) folded into a double string was in the middle PE-160 catheter to induce thrombosis. For sample administration, a saline-filled PE-60 catheter was cannulated to the exposed femoral vein. Different sample doses ($n = 9$ per dose) were administered through the PE-60 catheter cannulated to the femoral vein. After 15-min administration of sample, the shunt was opened for 5 min and then closed. Nylon strings were removed from the middle PE-160 catheter; the wet thrombus attached in the nylon strings was weighed.

Bleeding time

Bleeding time was assessed by a tail transection method (34–35). After treatments with either tested drugs or their vehicle, mice were maintained in a special immobilization cage that keeps the tail steady and immersed in 0.9% isotonic saline at 37°C. After 2 min, a distal 2-mm segment of the tail was severed with a razor blade. The tail was immediately reimmersed in warm saline with the tip of the tail 5 cm below the body. The bleeding time was defined as the time required for the stream of blood to cease. The end point was the arrest of bleeding lasting more than 30 s. All the experimental protocols to use animals were approved by the Animal Care and Use Committee at Kunming Institute of Zoology, Chinese Academy of Sciences.

Statistics

Data were analyzed by χ^2 and by *t*-test or repeated measure of analysis of variance (ANOVA).

RESULTS

Purification of Tablysin-15 from the horsefly SGE

As illustrated in Figure 1A, the supernatant of the horsefly SGE was divided into six fractions by Sephadex G-75 gel filtration consistent with our previous report (25). Fraction 3

was subjected to AKTA Mono S cationic exchange. By SDS-PAGE analysis, this peak displayed a single band under both reducing and non-reducing conditions, revealing that it is a homogeneous protein (named Tablysin-15) with a molecular weight of 26 kD (insert in Figure 1B).

Sequencing and cDNA cloning

N-terminus and peptide fragments of Tablysin-15 recovered from trypsin hydrolysis were sequenced by automated Edman degradation. Their sequences are shown unederlined in Figure 2. Based on the aa sequence of the N-terminus, a degenerated primer was designed to screen cDNA sequence encoding Tablysin-15. The complete cDNA sequence encoding Tablysin-15 was cloned from the horsefly salivary gland cDNA library (GenBank accession number GU363426). Tablysin-15 is composed of 255 aa including a predicted signal peptide (23 aa) and a mature protein (232 aa) (Figure 2). BLAST search indicated that Tablysin-15 shares sequence similarity to insect antigen 5 proteins. There is an Arg-Gly-Asp (RGD) sequence at the N-terminus of Tablysin-15. Similar to other platelet aggregation inhibitors such as variabilin (22), decorsin (36), ornatin (23), and snake disintegrins (37–39), the RGD sequence in Tablysin-15 is in a loop bracketed by cysteine residues (Figure 2B) but was found in the N-terminus of the protein. Next, Tablysin-15 clone was identified through screening of a cDNA library and cloning the corresponding sequence in an PET vector followed by transformation of E. coli as described in method. Purification of Tablysin-15 through different steps is shown in Figure 1C, with the resulting mature protein obtained after cleavage of the fusion protein with enterokinase, as depicted in lane 3.

Tablysin-15 inhibits platelet aggregation induced by agonists

RGD-containing proteins are well-known platelet aggregation inhibitors. Effects of Tablysin-15 on platelet aggregation induced by ADP, collagen and convulxin are illustrated in Figure 3A. Tablysin-15 strongly attenuated platelet aggregation induced by agonists without affecting the shape change.

Tablysin-15 inhibits thrombus formation under flow conditions

Collagen is a matrix protein that plays a pivotal role in the process of primary hemostasis; at sites of vascular injury, it initiates recruitment of circulating platelets and triggers a platelet activation cascade required to stimulate thrombus growth. We evaluated effects of Tablysin-15 on thrombus formation initiated by collagen under flow conditions. Figures 3B (panels b–d) demonstrate that Tablysin-15 dose-dependently inhibits thrombus formation at shear rates of 1500 s_{-1}; complete blockade was attained at ~ 3 μM inhibitor (Figure 3C). On the other hand, Tablysin-15 did not affect vWF-dependent platelet adhesion to collagen, which was characterized by single platelets bound to fibrillar collagen (Figure 3B, panel d).

Next, the effects of Tablysin-15 on platelet adhesion to immobilized matrix proteins were investigated. As illustrated in Figure 3C, different concentrations of Tablysin-15 dose-dependently inhibits platelet adhesion to fibronectin or fibrinogen but was without effect when soluble or fibrillar collagen was tested.

Tablysin-15 supports platelet adhesion and directly binds to integrin αIIbβ3

Figure 4A shows that immobilized Tablysin-15 at concentrations as low as 0.03 μg/ml support the adhesion of calcein-labeled platelets under static condition. Consistent with its disintegrin properties, platelet adhesion to immobilized Tablysin-15 was dose-dependently blocked by anti-integrin αIIbβ3 monoclonal antibody (abciximab), or by EDTA (Figure 4B). In an attempt to demonstrate direct interaction of Tablysin-15 to integrin αIIbβ3, the inhibitor was immobilized in microwell plates followed by addition of purified human

platelet αIIbβ3 and identification of the complex as described in the Methods section. Figure 4C illustrates that Tablysin-15 at 0.03 μg/well and above binds to purified αIIbβ3 at comparable level obtained with 3 μg/well of fibrinogen.

Tablysin-15 binding to platelets detected by flow cytometry

Platelet $\alpha_{IIb}\beta_3$ occupancy kits were used to detect Tablysin-15 binding to platelet integrin $\alpha_{IIb}\beta_3$. The fluorescence intensity is measured on a flow cytometer after addition of a staining reagent. This intensity is directly proportional to the number of monoclonal antibody (MAb) molecules bound on the platelet surface. Figure 5A and 5B respectively shows native or recombinant Tablysin-15 cause a dose-dependent shift of anti-integrin $\alpha_{IIb}\beta_3$ antibody fluorescence due to displacement by recombinant Tablysin-15. These results indicate that Tablysin and the anti-integrin antibody compete for the same binding site, *i.e.*, $\alpha_{IIb}\beta_3$

Tablysin-15 inhibits endothelial cell adhesion, proliferation and tube formation

In an attempt to estimate the specificity of Tablysin-15, it was added to endothelial cells which were then incubated with soluble collagen-, fibronectin- or vitronectin-coated wells. Figure 6A reveals that Tablysin-15 was exquisitely potent to block αvβ3 mediated adhesion to vitronectin with IC_{50} ~ 1 nM (Figure 6B). On the other hand, inhibition of α5β1-dependent MVEC adhesion to FNC was inhibited at much higher concentrations (IC_{50} ~ 1 μM), while no inhibition was attained for collagen (α2β1)-coated plates. It is concluded that Tablysin-15 readly recognizes both integrins $\alpha_{IIb}\beta_3$ and αvβ3. Control experiments with *Dipetalogater maxima* salivary gland antigen V (40) which was expressed and purified as Tablysin-15 did not show inhibition of adhesion at 3 μM (n=4, not shown).

Figure 6B shows that Tablysin-15 inhibits proliferation of MVEC in the presence of FBS and FGF with an IC_{50} of ~ 1 μM. Tablysin-15 also inhibits MVEC proliferation in the presence of FBS and single quotes (growth factors), but with a higher IC_{50} ~ 3 μM (not shown, n=5). Consistent with its antiangiogenic properties, Tablysin-15 prevents tube formation supported by GFR-matrigel; with 1 μM Tablysin-15 density of endothelial cells clusters were reduced, and tube formation was less abundant. At 3 μM, clusters of endothelial cells were no longer observable and tube formation was almost completely abolished (Figure 6C).

Anti-thrombotic activity *in vivo* and bleeding time evaluation

In the rat arteriovenous shunt thrombosis model, native and recombinant Tablysin-15, or urokinase, significantly inhibited thrombosis in a dose-dependent manner (Figure 7A). At the same molar concentration, native and recombinant Tablysin-15 had similar antithrombotic abilities, which was comparable to urokinase. At the dosage of 0.06 μmol/kg, they inhibited 70–85% thrombosis. Next, three concentrations of recombinant Tablysin-15 or urokinase (0.01, 0.05, and 0.1 μmol/kg) were administered to mice as described in Methods. Figure 7B shows that after 2-h treatment with Tablysin-15, the corresponding bleeding times were approximately 2.7, 3.5, and 5.8 min, respectively, while for urokinase it was about 4.2, 7.5, and 17.9 min. Next, the kinetics of bleeding time was performed for both Tablysin-15 and urokinase. Figure 7C shows that bleeding for Tablysin-15 was at maximum after 4 hrs, while for urokinase it took place at 8 hrs. After 16-h Tablysin-15 treatment, bleeding time had no obvious difference from the 0.9% NaCl treatment while for urokinase administration bleeding time was about 12.7 min after 20-h urokinase.

DISCUSSION

Disintegrins, a family of small (40–100 amino acids) cysteine-rich polypeptides that selectively block the adhesive function of integrin receptors, are released in the venoms of various vipers by proteolytic processing of PII SVMP precursors or are synthesized from short-coding mRNAs (7–11). While most disintegrins have been characterized in snake venoms, many have also been discovered in the saliva of blood sucking animals such as ticks, and leeches (18). However, existence of disintegrins in mosquitoes, bugs, or sand flies remained elusive thus far. Horseflies salivary gland contains bioactive compounds that affect the hemostatic system, and more than 30 peptides acting on the hemostatic system have been recently identified (26). In this report, a 26-kD protein named Tablysin-15 was purified and characterized as a novel disintegrin from the tabanide *T. yao*. Tablysin-15 does not share primary sequence homology to any RGD-containing molecules discovered so far; in addition, it displays 10 cysteines, and an RGD domain found in the N-terminus of the molecule. Tablysin-15 also differs from snake venom disintegrin since its mature form is not the result of processing of precursor as occurs with members of the ADAMs family identified in Viperidae (11). In this respect, it resembles short mRNA-coding disintegrins except that it has considerable higher *mol wt* and increased number of cysteines (7–11).

The RGD domain in Tablysin-15 is positioned in a loop bracketed by cysteine residues, implying that Tablysin-15 has the ability to bind to cellular integrins such as $\alpha_{IIb}\beta_3$ or endothelial cell $\alpha v\beta 3$. Accordingly, Tablysin-15 inhibits platelet aggregation by collagen, and ADP without interfering with shape change. It also inhibits platelet aggregation by convulxin, a potent platelet agonist which induces platelet aggregation independently of secondary mediators (41). Furthermore, Tablysin-15 inhibits thrombus formation under flow at high shear in a dose-dependent manner without interference in platelet adhesion to collagen fibrils. These results clearly indicate that a step distal to agonist-induced platelet activation, such as integrin-mediated platelet aggregation, was the target of Tablysin-15. As a consequence, the pro-hemostatic functions of platelet are attenuated which translate in abrogation of thrombus formation. Consistent with this property immobilized Tablysin-15 supports platelet adhesion by a mechanism which is blocked by anti-integrin $\alpha_{IIb}\beta_3$ monoclonal antibody (*e.g.* abciximab), or by EDTA. Further, solid-phase assays and flow cytometry demonstrate binding of human platelet integrin $\alpha_{IIb}\beta_3$ to Tablysin-15. It is concluded that Tablysin-15 belongs to a novel family of disintegrins which target $\alpha_{IIb}\beta_3$.

Platelet integrins and fibrinogen are two key components in thrombosis. Fibrinogen binds to the receptor $\alpha_{IIb}\beta_3$ to induce platelet aggregation and is also critical for stable clot formation. Experiments performed *in vivo* indicated that Tablysin-15 had strong anti-thrombotic property which was comparable to urokinase, which was used herein as a positive control. However, and in contrast to urokinase, mice injected with Tablysin-15 displayed less bleeding. Even at Tablysin-15 dose (~ 1 mg/kg) that inhibits 90% thrombosis, bleeding time was approximately 5.9 min while for urokinase it was 12.7 min. The differences observed for bleeding time after administration of urokinase or Tablysin-15 appears to be due to the relative contribution of their respective mechanism of action in the inhibition of thrombus formation; generation of plasmin by the former and the blockade of receptor occupancy by the latter. The effects of Tablysin-15 in thrombus formation *in vivo* resemble the activity of other sialogenins which block platelet aggregation *in vivo* through antagonism of integrin $\alpha_{IIb}\beta_3$ such as decorsin from leech *Macrobdella decora* (24). It also resembles trigamin from *Trimerusurus gramineus*, or echistatin from *Echis carinatus* snake venoms which are effective antithrombotics according to different experimental models (4). Notably, disintegrins from exogenous sources have been instrumental in the development of novel therapeutics to treat cardiovascular diseases. For example, epitifibatide (integrilin) is based on the structure of a functional and structural loop present in a disintegrin from

Sistrurus m. barbori that was specific for $\alpha_{IIb}\beta_3$. It has become a very effective drug for preventing thrombus formation leading to occlusion of vessels and stents after surgery by preventing fibrinogen and fibrin binding to activated $\alpha_{IIb}\beta_3$ on platelets (42). Further, tirofiban (Aggrastat) is a non-peptidic $\alpha_{IIb}\beta_3$ inhibitor designed based on echistatin, a disintegrin which like Tablysin-15 blocks both αvβ3 and $\alpha_{IIb}\beta_3$ (4). Of note, control experiments indicated that Tablysin-15 did not activate plasminogen or hydrolyzed fibrinogen (not shown) indicating that anti-thrombotic property of Tablysin-15 is due to inhibition of platelet aggregation.

Our cell adhesion assays demonstrated inhibition of MVEC adhesion to VTNC at very low concentrations of Tablysin-15. This finding is particularly important because among members of the integrin family, a prominent role in angiogenesis and metastatic dissemination is played by αvβ3, which, according to in vivo angiogenesis is required for basic fibroblast growth factoRinduced angiogenesis (43). Tablysin-15 also inhibits MVEC proliferation in the presence of FGF suggesting that it might affect survival mechanisms or signaling pathways of endothelial cell (43–44). Consistent with these activities, Tablysin-15 effectively blocks matrigel-supported tube formation *in vitro*. The specific of Tablysin-15 towards integrin αvβ3 is particularly important since it is strongly up-regulated at transcriptional level by proangiogenic growth factors or chemokines in activated endothelial cells. Expression and activation of this integrin was also found to be correlated with tumor invasion and metastases in melanomas, gliomas, ovarian, and breast cancer (12–15). Furthermore, activated αvβ3 is reported to cooperate with metalloproteinase and to strongly promote metastasis in human breast cancer cells (16, 17). It is important to recognize that a number of αvβ3 antagonists, including antibodies, peptidomimetics, and cyclic RGD peptides, have been developed and are currently used in clinical trials to inhibit αvβ3-mediated processes and to visualize tumor angiogenesis and metastases. Among these compounds, monoclonal antibodies, such as LM609 or its humanized version Vitaxin, can effectively bind to αvβ3 (43, 45). Accordingly, Tablysin-15 emerges as a novel tool to understand the function of integrin αvβ3 and may be useful as a therapeutic agent, or for imaging purposes toward tumor visualization and location (3). These results thus highlight the diversity of disintegrins in exogenous secretions in one hand, and angiogenesis inhibition as an important biological function in the saliva of hematophagous animals, in the other (31). Due to its unique positioning of the functional RGD motif, Tablysin-15 presents a novel template to study the structure-function relationship of disintegrins blockade and inhibition of platelet function and potential use in pathological condition with abnormal platelet aggregation, or angiogenesis (46–50). Solving the three-dimensional structures of Tablysin-15 will likely reveal how its unique RGD motif negatively modulates $\alpha_{IIb}\beta_3$ function.

Acknowledgments

The authors thank NIAID intramural editor Brenda Rae Marshall for assistance.

This work was supported by the Chinese National Natural Science Foundation (30830021 and 30800185), the Chinese Ministry of Science and Technology (2010CB529800) and the Intramural Research Program of the Division of Intramural Research, National Institute of Allergy and Infectious Diseases, National Institutes of Health.

REFERENCES

1. Avraamides CJ, Garmy-Susini B, Varner JA. Integrins in angiogenesis and lymphangiogenesis. Nat Rev Cancer. 2008 Aug; 8(8):604–617. [PubMed: 18497750]
2. Hood JD, Cheresh DA. Role of integrins in cell invasion and migration. Nat Rev Cancer. 2002 Feb; 2(2):91–100. [PubMed: 12635172]
3. Zannetti A, Del Vecchio S, Iommelli F, et al. Imaging of alpha(v)beta(3) expression by a bifunctional chimeric RGD peptide not cross-reacting with alpha(v)beta(5). Clin Cancer Res. 2009 Aug 15; 15(16):5224–5233. [PubMed: 19671851]
4. Huang TF. What have snakes taught us about integrins? Cell Mol Life Sci. 1998 Jun; 54(6):527–540. [PubMed: 9676572]
5. Markland FS. Snake venoms and the hemostatic system. Toxicon. 1998 Dec; 36(12):1749–1800. [PubMed: 9839663]
6. Calvete JJ. Structure-function correlations of snake venom disintegrins. Curr Pharm Des. 2005; 11(7):829–835. [PubMed: 15777237]
7. Rahman S, Flynn G, Aitken A, et al. Differential recognition of snake venom proteins expressing specific Arg-Gly-Asp (RGD) sequence motifs by wild-type and variant integrin alphaIIbbeta3: further evidence for distinct sites of RGD ligand recognition exhibiting negative allostery. Biochem J. 2000 Feb 1; 345(Pt 3):701–709. [PubMed: 10642531]
8. Lu X, Lu D, Scully MF, et al. Structure-activity relationship studies on ADAM protein-integrin interactions. Cardiovasc Hematol Agents Med Chem. 2007 Jan; 5(1):29–42. [PubMed: 17266546]
9. Sanz L, Bazaa A, Marrakchi N, et al. Molecular cloning of disintegrins from Cerastes vipera and Macrovipera lebetina transmediterranea venom gland cDNA libraries: insight into the evolution of the snake venom integrin-inhibition system. Biochem J. 2006 Apr 15; 395(2):385–392. [PubMed: 16411889]
10. Fox JW, Serrano SM. Insights into and speculations about snake venom metalloproteinase (SVMP) synthesis, folding and disulfide bond formation and their contribution to venom complexity. FEBS J. 2008 Jun; 275(12):3016–3030. [PubMed: 18479462]
11. Kini RM, Evans HJ. Structural domains in venom proteins: evidence that metalloproteinases and nonenzymatic platelet aggregation inhibitors (disintegrins) from snake venoms are derived by proteolysis from a common precursor. Toxicon. 1992 Mar; 30(3):265–293. [PubMed: 1529462]
12. Watson SP, Auger JM, McCarty OJ, et al. GPVI and integrin alphaIIb beta3 signaling in platelets. J Thromb Haemost. 2005 Aug; 3(8):1752–1762. [PubMed: 16102042]
13. Ludwig IS, Geijtenbeek TB, van Kooyk Y. Two way communication between neutrophils and dendritic cells. Curr Opin Pharmacol. 2006 Aug; 6(4):408–413. [PubMed: 16750420]
14. Silva R, D'Amico G, Hodivala-Dilke KM, et al. Integrins: the keys to unlocking angiogenesis. Arterioscler Thromb Vasc Biol. 2008 Oct; 28(10):1703–1713. [PubMed: 18658045]
15. Jackson SP, Schoenwaelder SM. Antiplatelet therapy: in search of the 'magic bullet'. Nat Rev Drug Discov. 2003 Oct; 2(10):775–789. [PubMed: 14526381]
16. McLane MA, Marcinkiewicz C, Vijay-Kumar S, et al. Viper venom disintegrins and related molecules. Proc Soc Exp Biol Med. 1998 Nov; 219(2):109–119. [PubMed: 9790167]
17. Swenson S, Ramu S, Markland FS. Anti-angiogenesis and RGD-containing snake venom disintegrins. Curr Pharm Des. 2007; 13(28):2860–2871. [PubMed: 17979731]
18. Francischetti IM. Platelet aggregation inhibitors from hematophagous animals. Toxicon. 2010 Dec 15; 56(7):1130–1144. [PubMed: 20035779]
19. Ribeiro JM, Francischetti IM. Role of arthropod saliva in blood feeding: sialome and post-sialome perspectives. Annu Rev Entomol. 2003; 48:73–88. [PubMed: 12194906]
20. Francischetti IM, Sa-Nunes A, Mans BJ, et al. The role of saliva in tick feeding. Front Biosci. 2009; 14:2051–2088. [PubMed: 19273185]
21. Mans BJ, Louw AI, Neitz AW. Savignygrin, a platelet aggregation inhibitor from the soft tick Ornithodoros savignyi, presents the RGD integrin recognition motif on the Kunitz-BPTI fold. J Biol Chem. 2002 Jun 14; 277(24):21371–21378. [PubMed: 11932256]

22. Wang X, Coons LB, Taylor DB, et al. Variabilin, a novel RGD-containing antagonist of glycoprotein IIb-IIIa and platelet aggregation inhibitor from the hard tick Dermacentor variabilis. J Biol Chem. 1996 Jul 26; 271(30):17785–17790. [PubMed: 8663513]
23. Mazur P, Henzel WJ, Seymour JL, et al. Ornatins: potent glycoprotein IIb-IIIa antagonists and platelet aggregation inhibitors from the leech Placobdella ornata. Eur J Biochem. 1991 Dec 18; 202(3):1073–1082. [PubMed: 1765068]
24. McLane MA, Gabbeta J, Rao AK, et al. A comparison of the effect of decorsin and two disintegrins, albolabrin and eristostatin, on platelet function. Thromb Haemost. 1995 Nov; 74(5): 1316–1322. [PubMed: 8607116]
25. Xu X, Yang H, Ma D, et al. Toward an understanding of the molecular mechanism for successful blood feeding by coupling proteomics analysis with pharmacological testing of horsefly salivary glands. Mol Cell Proteomics. 2008 Mar; 7(3):582–590. [PubMed: 18087067]
26. Ma D, Wang Y, Yang H, et al. Anti-thrombosis repertoire of blood-feeding horsefly salivary glands. Mol Cell Proteomics. 2009 Sep; 8(9):2071–2079. [PubMed: 19531497]
27. Francischetti IM, Saliou B, Leduc M, et al. Convulxin, a potent platelet-aggregating protein from Crotalus durissus terrificus venom, specifically binds to platelets. Toxicon. 1997 Aug; 35(8):1217–1228. [PubMed: 9278971]
28. Calvo E, Tokumasu F, Marinotti O, et al. Aegyptin, a novel mosquito salivary gland protein, specifically binds to collagen and prevents its interaction with platelet glycoprotein VI, integrin alpha2beta1, and von Willebrand factor. J Biol Chem. 2007 Sep 14; 282(37):26928–26938. [PubMed: 17650501]
29. Quinn M, Deering A, Stewart M, et al. Quantifying GPIIb/IIIa receptor binding using 2 monoclonal antibodies: discriminating abciximab and small molecular weight antagonists. Circulation. 1999 May 4; 99(17):2231–2238. [PubMed: 10226086]
30. Chang SJ, Chang CN, Chen CW. Occupancy of glycoprotein IIb/IIIa by B-6 vitamers inhibits human platelet aggregation. J Nutr. 2002 Dec; 132(12):3603–3606. [PubMed: 12468595]
31. Francischetti IM, Mather TN, Ribeiro JM. Tick saliva is a potent inhibitor of endothelial cell proliferation and angiogenesis. Thromb Haemost. 2005 Jul; 94(1):167–174. [PubMed: 16113800]
32. Assumpcao TC, Alvarenga PH, Ribeiro JM, et al. Dipetalodipin, a novel multifunctional salivary lipocalin that inhibits platelet aggregation, vasoconstriction, and angiogenesis through unique binding specificity for TXA2, PGF2alpha, and 15(S)-HETE. J Biol Chem. 2010 Dec 10; 285(50): 39001–39012. [PubMed: 20889972]
33. Sperzel M, Huetter J. Evaluation of aprotinin and tranexamic acid in different in vitro and in vivo models of fibrinolysis, coagulation and thrombus formation. J Thromb Haemost. 2007 Oct; 5(10): 2113–2118. [PubMed: 17666018]
34. Dejana E, Villa S, de Gaetano G. Bleeding time in rats: a comparison of different experimental conditions. Thromb Haemost. 1982 Aug 24; 48(1):108–111. [PubMed: 6753230]
35. Subramaniam M, Frenette PS, Saffaripour S, et al. Defects in hemostasis in P-selectin-deficient mice. Blood. 1996 Feb 15; 87(4):1238–1242. [PubMed: 8608210]
36. Seymour JL, Henzel WJ, Nevins B, et al. Decorsin. A potent glycoprotein IIb-IIIa antagonist and platelet aggregation inhibitor from the leech Macrobdella decora. J Biol Chem. 1990 Jun 15; 265(17):10143–10147. [PubMed: 2351655]
37. Gould RJ, Polokoff MA, Friedman PA, et al. Disintegrins: a family of integrin inhibitory proteins from viper venoms. Proc Soc Exp Biol Med. 1990 Nov; 195(2):168–171. [PubMed: 2236100]
38. Blobel CP, White JM. Structure, function and evolutionary relationship of proteins containing a disintegrin domain. Curr Opin Cell Biol. 1992 Oct; 4(5):760–765. [PubMed: 1419054]
39. Scarborough RM, Rose JW, Naughton MA, et al. Characterization of the integrin specificities of disintegrins isolated from American pit viper venoms. J Biol Chem. 1993 Jan 15; 268(2):1058–1065. [PubMed: 8419314]
40. Assumpcao TC, Charneau S, Santiago PB, et al. Insight into the Salivary Transcriptome and Proteome of Dipetalogaster maxima. J Proteome Res. 2011 Jan 4.
41. Faili A, Randon J, Francischetti IM, et al. Convulxin-induced platelet aggregation is accompanied by a powerful activation of the phospholipase C pathway. Biochem J. 1994 Feb 15; 298(Pt 1):87–91. [PubMed: 8129734]

42. Clemetson, KJ.; Kini, RM. Introduction. Toxins and Hemostasis From bench to bedside. Kini, RM.; Clemetson, KJ.; Markland, FS.; McLane, MA.; Morita, T., editors. Springer; 2010. p. 1-9. (Springer.)
43. Cheresh DA, Stupack DG. Regulation of angiogenesis: apoptotic cues from the ECM. Oncogene. 2008 Oct 20; 27(48):6285–6298. [PubMed: 18931694]
44. Shattil SJ, Kim C, Ginsberg MH. The final steps of integrin activation: the end game. Nat Rev Mol Cell Biol. 2010 Apr; 11(4):288–300. [PubMed: 20308986]
45. Griffioen AW, Vyth-Dreese FA. Angiostasis as a way to improve immunotherapy. Thromb Haemost. 2009 Jun; 101(6):1025–1031. [PubMed: 19492143]
46. Marcinkiewicz C. Functional characteristic of snake venom disintegrins: potential therapeutic implication. Curr Pharm Des. 2005; 11(7):815–827. [PubMed: 15777236]
47. Munnix IC, Cosemans JM, Auger JM, et al. Platelet response heterogeneity in thrombus formation. Thromb Haemost. 2009 Dec; 102(6):1149–1156. [PubMed: 19967145]
48. Watson SP. Platelet activation by extracellular matrix proteins in haemostasis and thrombosis. Curr Pharm Des. 2009; 15(12):1358–1372. [PubMed: 19355974]
49. Jennings LK. Mechanisms of platelet activation: need for new strategies to protect against platelet-mediated atherothrombosis. Thromb Haemost. 2009 Aug; 102(2):248–257. [PubMed: 19652875]
50. Francischetti IM, Seydel KB, Monteiro RQ. Blood coagulation, inflammation, and malaria. Microcirculation. 2008 Feb; 15(2):81–107. [PubMed: 18260002]

What is known about this topic?

Disintegrins are a family of small cysteine-rich polypeptides which display series of biological functions associated with cell-cell interaction, cell adhesion and migration and angiogenesis. They are mostly found in snake venoms, but so far only sources of disintegrins in blood-sucking animals were ticks and leeches.

What does this paper add?

Tablysin-15 is a novel family of disintegrins, the first found in horseflies that display unique positioning of the functional RGD motif which was characterized as a platelet antagonist of integrins αIIbβ3 and αvβ3. Therefore, it represents a novel template to study the structure-function relationship of disintegrins blockade and inhibition of platelet function and angiogenesis.

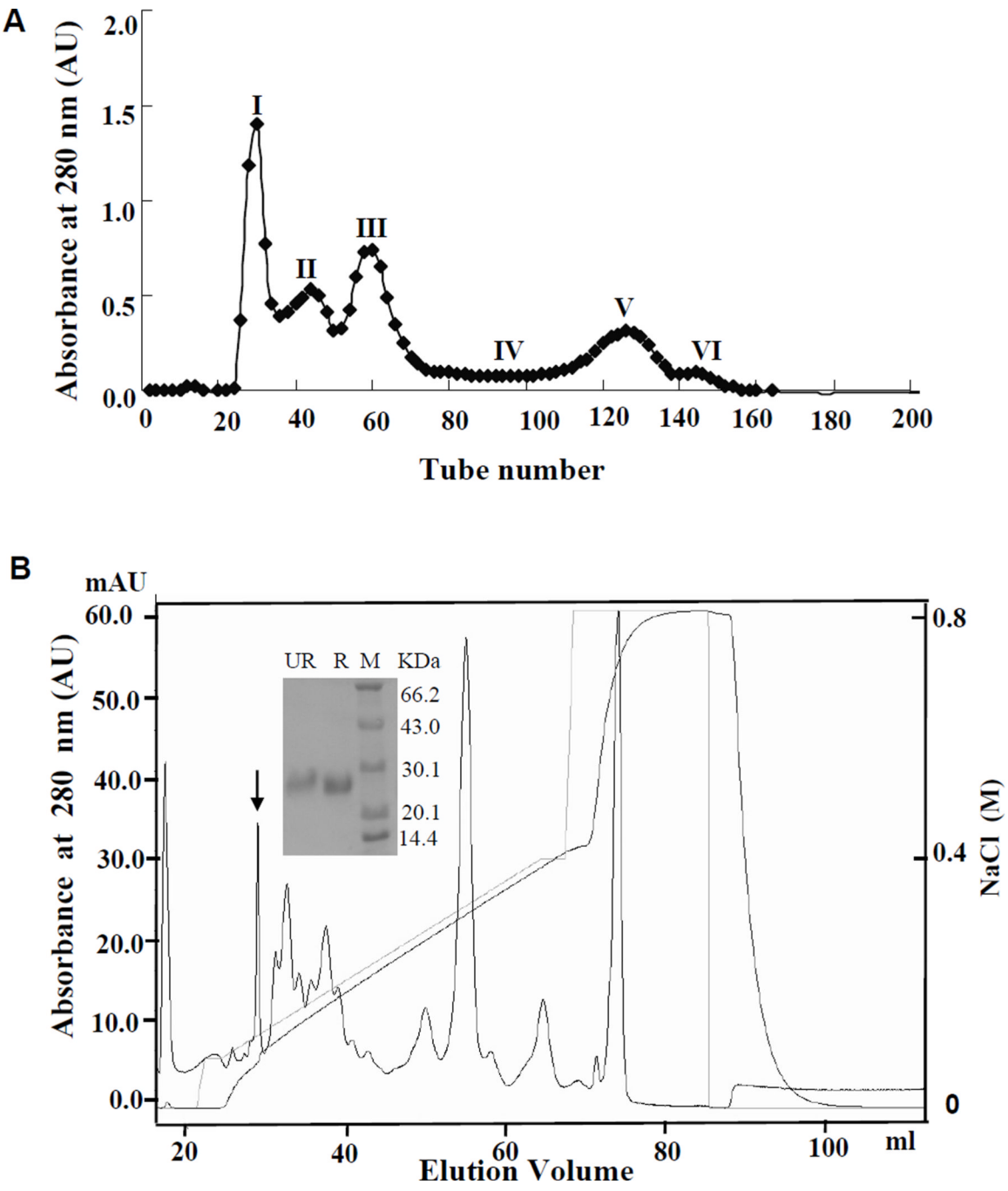

Figure 1. Purification of Tablysin-15 from the horsefly salivary gland extract (SGE)

(A) SGE aliquot of 0.41 g was dissolved in 10 mL 0.1 M PBS, pH 6.0, and then was applied to a Sephadex G-75 (Superfine; Amersham Biosciences, Arlington Heights, IL) 2.6 × 100-cm gel filtration column equilibrated with 0.1 M PBS. Elution was performed with the same buffer, collecting fractions of 3.0 mL. The absorbance of the eluate was monitored at 280 nm. (B) Fraction 3 from Figure 1A was subjected to AKTA Mono S cationic exchange equilibrated with 0.02 M PBS, pH 6.0. The elution was performed at a flow rate of 1 ml/min with the indicated NaCl gradient. Inset in Figure 1B: SDS-PAGE analysis of fraction containing platelet-inhibitory properties. R, reduced; UR, non-reduced; M, molecular weight marker.

A

```
atgacttccataccggtgtccagctttttacttgcggccttagtactacaatacgccact  60
 M  T  S  I  P  V  S  S  F  L  L  A  A  L  V  L  Q  Y  A  T   20
agcgacgcagttaactactgtagattgccttgtcgagggataattaccatgtgggctgt 120
 S  D  A  V  N  Y  C  R  L  P  C  R  G  D  N  Y  H  V  G  C   40
ggtgagccagcgtatgcccaggaatgtgggcaaagtccaagaactcgcgagttattgaag 180
 G  E  P  A  Y  A  Q  E  C  G  Q  S  P  R  T  R  E  L  L  K   60
gagcatagaaatgagattttgtcgaagatcaacgatgtgcgagaccatgtggccaaggga 240
 E  H  R  N  E  I  L  S  K  I  N  D  V  R  D  H  V  A  K  G   80
tcatgggactaccagtggcagcccgaatgaaagttgttgtatgggatgcggaactcgct 300
 S  W  G  L  P  V  A  A  R  M  K  V  V  V  W  D  A  E  L  A  100
ggtttagccaaacgacatacaaagggatgcgttggagagacacatgcgtgtcgaaacaca 360
 G  L  A  K  R  H  T  K  G  C  V  G  E  T  H  A  C  R  N  T  120
gaacgtttctggttgccaggtcaactaaacttcaaatactccggcgacaagctaccccgc 420
 E  R  F  W  L  P  G  Q  L  N  F  K  Y  S  G  D  K  L  P  R  140
attaaggaacttattgatgatgctgtcaaaaaaggccacttgcagaagcataatattacg 480
 I  K  E  L  I  D  D  A  V  K  K  G  H  L  Q  K  H  N  I  T  160
agagaaattatagggaactatagggagaatggacctaatggggatgtcaaggaacttgcc 540
 R  E  I  I  G  N  Y  R  E  N  G  P  N  G  D  V  K  E  L  A  180
ttggccatatctgatcgagtcaccgccgttggctgcggactaactacttggcaggatgga 600
 L  A  I  S  D  R  V  T  A  V  G  C  G  L  T  T  W  Q  D  G  200
gcaaaggctcgcgcacttcttacgtgtaacttctcctcgcagaacactcggggtcgacct 660
 A  K  A  R  A  L  L  T  C  N  F  S  S  Q  N  T  R  G  R  P  220
gtctacaaaatcggcaatagtcctggcgaaaagtgcatcgagaaggatgaaacgtataaa 720
 V  Y  K  I  G  N  S  P  G  E  K  C  I  E  K  D  E  T  Y  K  240
aacttgtgccctgctactgaacctatcgaccctaataagtctaactagcgtcatgtatct 780
 N  L  C  P  A  T  E  P  I  D  P  N  K  S  N  *              255
atgtatataaataaaattgaagtgtctgtctgtaatataaaacaactgtcacttattgag 840

cgcaaaaaaaaaaaaaaaaaaaaaaaaaaaa
```

B

```
Tablysin 15 VNYCRLPCRGDNYHVGCGEPAYAQECGQSPRTRELLKEHRNE…
Ornatin      IPQCRDVKESGQPNDKCRCNGKPCTVGKCTIARGDDNDKCT   41
Decorsin       APRLPQCQGDDQEKCLCNKDECPPGQCRFPRGDADPYCE   39
Variabilin   NTFSDENPGFPCDCTSADAKRACGIQCACWPRGDTPGGGRRIIDGQQ   47
Barbourin  EAGEECDCGSPENPCCDAATCKLRPGAQCADGLCCDQCRFMKKGTVCRVAKGDWNDDTC…
Savignygrin YQPECLEPSLYGCRGDEDATFGWTFDREDGGCRQGSYCTRFGQPKNYFRSERDCKKAC…
```

C

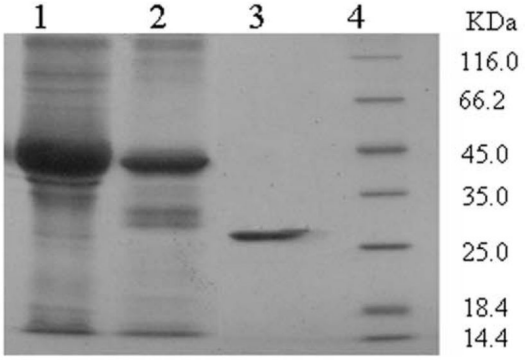

Figure 2. cDNA encoding Tablysin-15 and deduced amino acid (aa) sequence

(A) The aa sequences of peptide fragments determined by Edman degradation are underlined. The predicted signal peptide is *italic*. *, stop codon. (B) Comparison of the N-terminal partial aa sequence of Tablysin-15 with other disintegrins from arthropods saliva and snakes venoms. RGD or KGD sequences are **bold**. (C) SDS-PAGE analysis of recombinant Tablysin-15. Lane1: The lysate of inclusion bodies of recombinant Tablysin-15 were solubilized in 20 mM Tris–HCl, pH 7.9 with 6 M urea. Lane 2: The elute of recombinant Tablysin-15 inclusion bodies lysate from the Ni-NTA resin. Lane 3: Purified

recombinant Tablysin-15 after AKTA Mono S chromatography. Lane 4: molecular weight marker. All these samples were subjected to reduced SDS-PAGE.

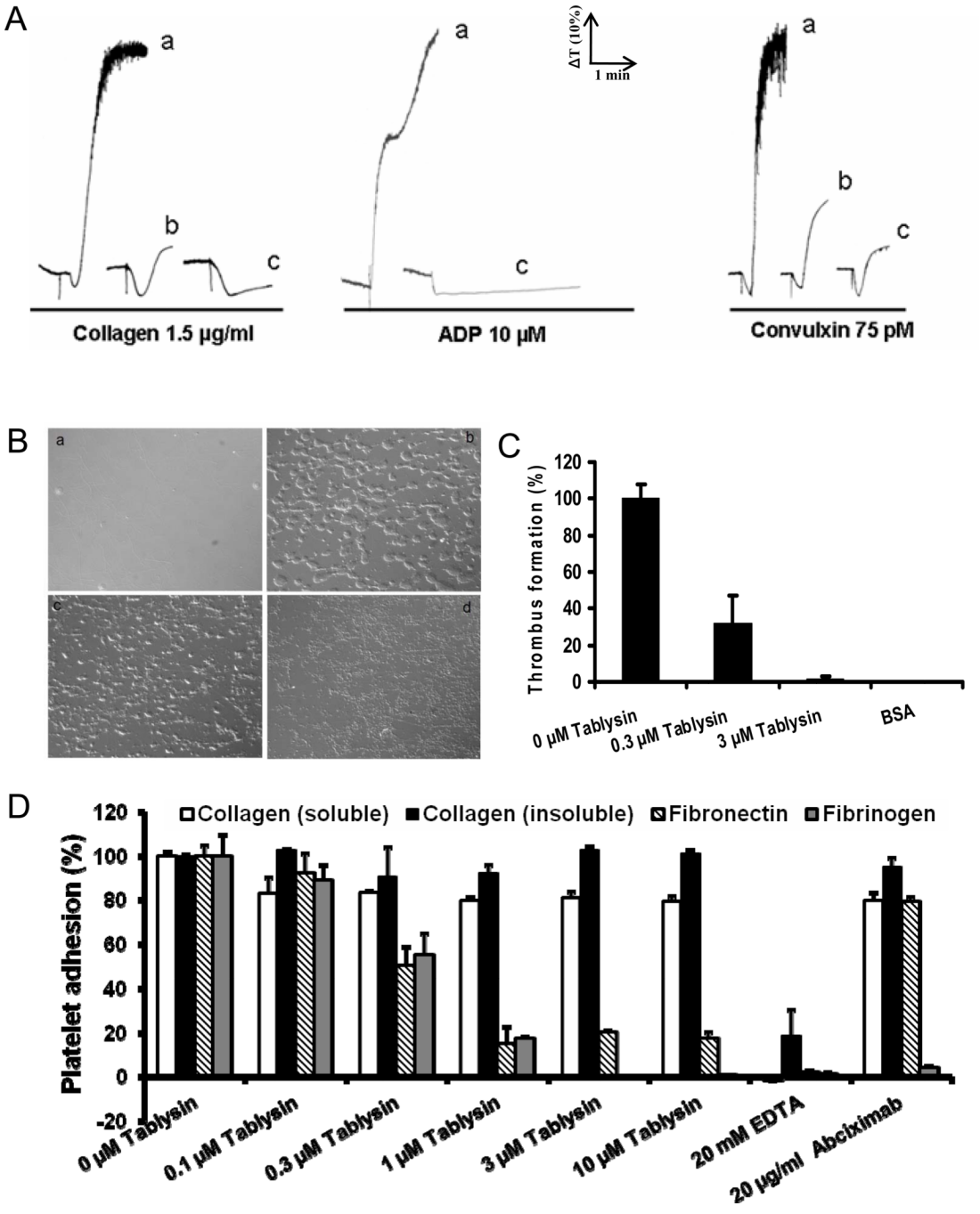

Figure 3. Interactions of Tablysin-15 and platelets

(A) Tablysin-15 inhibits human platelet aggregation induced by collagen, ADP and convulxin. Human platelet-rich plasma (2×10^5/µl) was incubated with Tablysin-15 (tracings *a*, 0 nM; *b*, 85 nM; *c*, 670 nM) for 1 min followed by addition of platelet agonists as indicated. Platelet aggregation was estimated by turbidimetry under test tube stirring conditions. The tracings represent a typical experiment. (B) Tablysin-15 inhibits thrombus formation under flow conditions. Anticoagulated (PPACK) whole blood was perfused over immobilized fibrillar collagen for 240 s at a shear rate of 1500 s^{-1} in the presence of 0 (panel b), 0.3 (panel c), and 3.0 µM (panel d) of Tablysin-15; panel a is a collagen-coated slides without perfused blood. (C) Dose-response curve for Tablysin-15 inhibition of

thrombus formation under flow conditions. (D) Tablysin-15 (0–10 μM) inhibit platelet adhesion to fibronectin, human fibrinogen, without significant effects on adhesion to soluble or fibrillar collagen. EDTA (20 mM) and abciximab (20 μg/mL) were used as controls. Experiments were repeated 3–4 times.

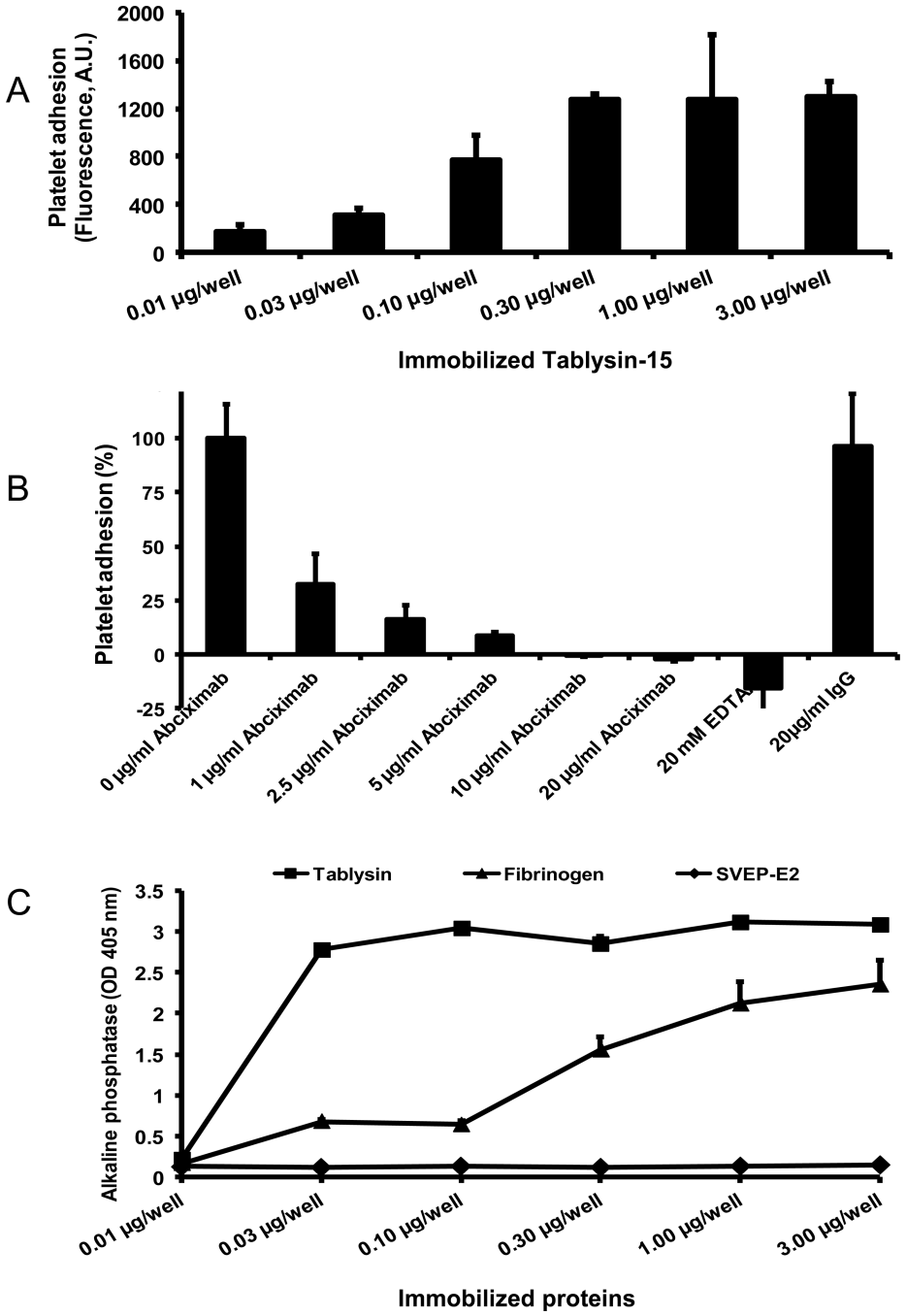

Figure 4. Interactions of Tablysin-15 and platelet integrin αIIbβ3

(A) Platelets adhere to Tablysin-15 coated in a 96-well plate with concentration range from 0.01 μg/well to 3 μg/well ($n = 5$). (B) Different concentrations of abciximab (0–20 μg/mL) markedly inhibit platelet adhesion to 2 μg of Tablysin-15-coated wells. Controls included EDTA and mouse isotype IgG. (C) Solid-phase assays shows integrin αIIbβ3 binding to immobilized Tablysin-15 and fibrinogen but not to SVEP-E2 (*E. coli*-expressed salivary protein). Purified human platelet αIIbβ3 was added to each well followed by detection with mouse anti-human integrin β3 antibody. BSA was used as negative control. All experiments were performed in triplicates.

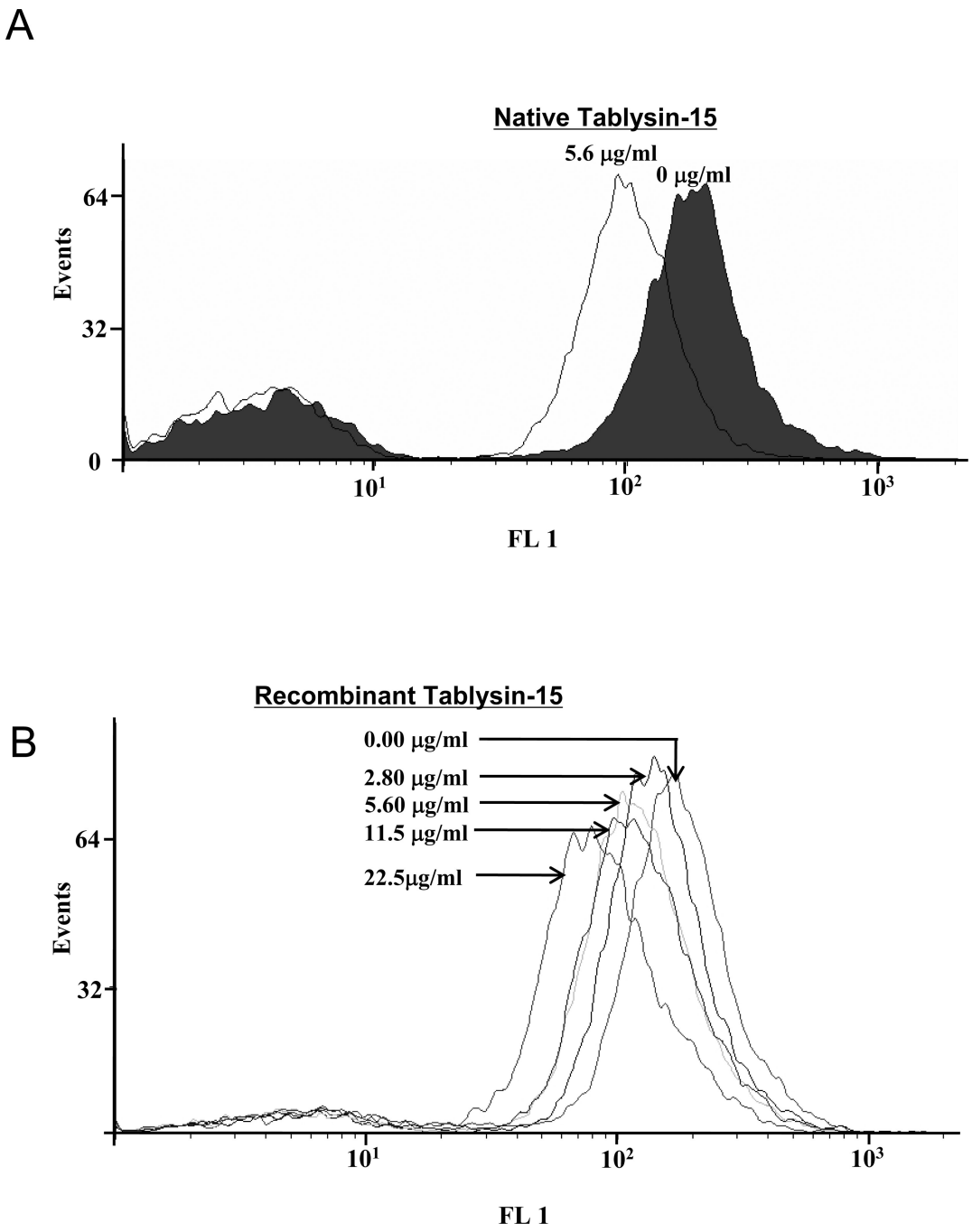

Figure 5. Platelet $\alpha_{IIb}\beta_3$ receptors are occupied by Tablysin-15 analyzed by flow cytometry

(A) Native Tablysin-15 occupies platelet $\alpha_{IIb}\beta_3$ receptor; (B) Recombinant Tablysin-15 occupies platelet $\alpha_{IIb}\beta_3$ receptor in a dose–dependent manner (n = 5). The values for numbers of free platelet $\alpha_{IIb}\beta_3$ treated by Tablysin-15 are significant different from the value for the control (*P < 0.05 and **p < 0.01).

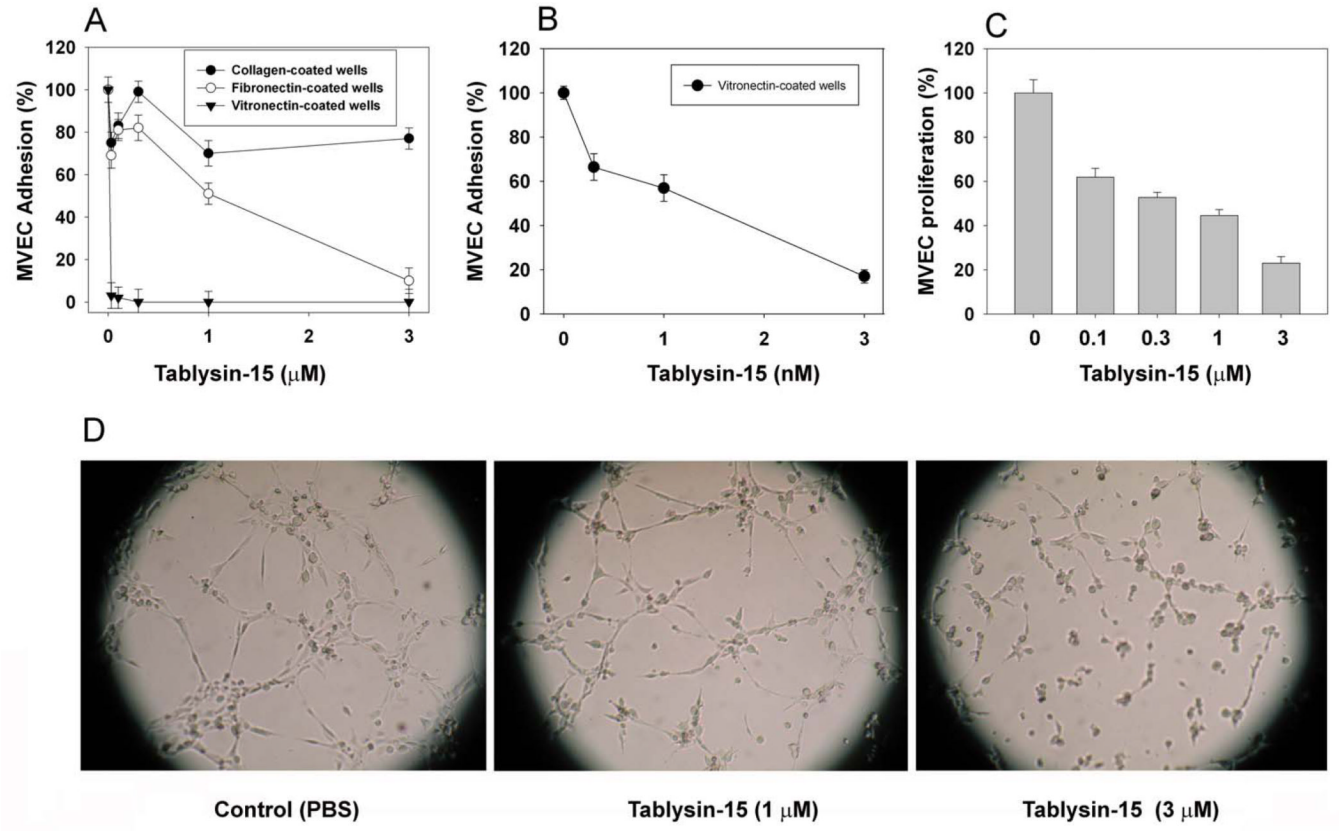

Figure 6. Anti-angiogenesis properties of Tablysin-15

(A) Tablysin-15 was incubated with MVEC and the mixture added to vitronectin-, fibronectin-, or soluble collagen-coated wells. (B) Tablysin-15 was added to MVEC in the presence of FBS and FGF and proliferation was estimated 72 hrs after with MTT. (C) Tube formation was estimated as described in Methods using growth-factor reduced matrigel. Experiments were performed in quadruplicates or quintuplicates.

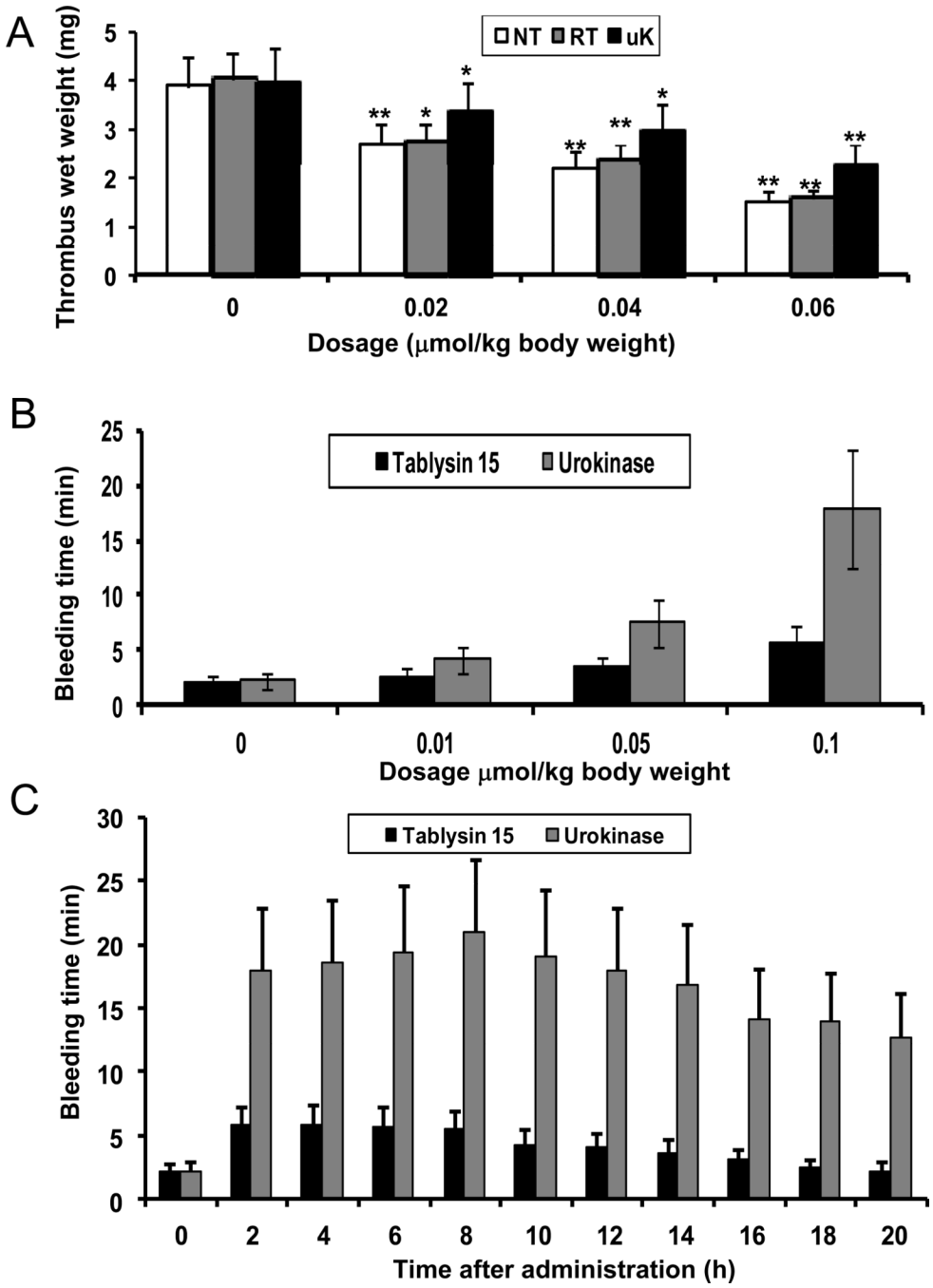

Figure 7. Antithrombotic activities of Tablysin-15 *in vivo*

(A) Antithrombotic effects of native and recombinant Tablysin-15, or urokinase in the rat arteriovenous shunt thrombosis model. Bleeding time induced by intravenous injection of Tablysin-15 was evaluated in dose- (B) and time-dependent manners (C). Experiments were performed as described in NT, native Tablysin-15; RT, recombinant Tablysin-15; UK, urokinase. Methods (*, $P < 0.05$; **, $P < 0.01$).